Enhanced Velocity Estimation using Gridded Tomography in Complex Chalk

By

Mick Sugrue[1]
Ian F. Jones[1]
Emma Evans[1]
Stuart Fairhead[2]
Gary Marsden[3]

1: GX Technology,, 180 High Street, Egham, Surrey TW20 9DN, UK
2: Amerada Hess Corporation, USA
3: Amerada Hess A/S, Denmark

Geophysical Prospecting, 2004, v52, No.6, p683-691.

Corresponding Author
Ian F. Jones
ijones@gxt.com

Enhanced Velocity Estimation using Gridded Tomography in Complex Chalk

Mick Sugrue[1], Ian F. Jones[1], Emma Evans[1], Stuart Fairhead[2], Gary Marsden[3]

1: GX Technology, 180 High Street, Egham, Surrey TW20 9DN, UK
2: Amerada Hess Corporation, USA
3: Amerada Hess A/S, Denmark

Abstract
The theme of the 2003 EAGE/SEG imaging workshop concerned the contrast between different philosophies of 'model building': whether an explicit, user determined model should be imposed throughout the processing, with user updates at each step; or alternatively, whether user intervention should be kept to a minimum so as to avoid preconceived bias, and instead to allow the data itself to guide some heuristic process to converge to an optimal solution.

Here we consider a North Sea study where our initial approach was to build the subsurface model using interpreted horizons as a guide to the velocity update. This is common practice in the North Sea, where the geology 'lends itself' to a layer-based model representation. In other words, we encourage preconceived bias, as we consider it to be a meaningful geological constraint on the solution.

However, in this instance we had a thick chalk sequence, wherein the vertical compaction gradient changed subtlety, in a way not readily discernable from the seismic reflection data. As a consequence, imposing the explicit top and bottom chalk horizons, with an intervening vertical compaction gradient (of the form $v(x,y,z) = v_0(x,y) + k(x,y).z$), led to a misrepresentation of the subsurface.

To address this issue, a gridded model building approach was also tried. This relied on dense continuous automatic picking of residual moveout in CRP gathers at each iteration of the model update, followed by gridded tomography, resulting in a smoothly varying velocity field which was able to reveal the underlying local changes within the chalk.

Introduction
Current practice in velocity model building usually resorts to one of two approaches: the layer-based and the gridded (Jones, 2003). The layer-based approach is typical of say a North Sea type environment, where sedimentary interfaces delimit changes in the velocity field. The gridded approach is adopted in environments such as found in the Gulf of Mexico, where the velocity regime is decoupled from the sedimentation, and is governed primarily by vertical compaction gradients (velocity increasing with depth), controlled by de-watering, with iso-velocity contours sub-paralleling the sea bed.

In the example considered here, which is typical of many North Sea fields, we have a thick chalk sequence, with a vertical compaction gradient within the chalk. The nature of these compaction gradients can be quite complex, with many subdivisions that are not obviously manifest in terms of a clear and laterally continuous seismic response. Due to compaction within the chalk, we can move from a near constant velocity regime in the uppermost part of the chalk, to a steep compaction gradient regime, and then back to a constant (high) velocity region at the base of the chalk, where the chalk has been compressed as much as it can be by the overburden pressure.

Two classes of error can occur in building a model for such chalk bodies:

1. The internal layering in the chalk may not be sufficiently well represented in the layered model, due to the difficulty in picking a clear event when we have a change in compaction gradient rather than a sharp change in reflectivity

2. Errors in the estimate of the values for the compaction gradient can manifest themselves as apparent anisotropy (Alkhalifa, 1997; Jones, et al, 2003)

Both of these errors will result in sub-optimal imaging, including the lateral mispositioning of faults (Alkhalifa & Tsvankin, 1995; Hawkins, et al, 2001).

North Sea Example

The real data shown here come from the South Arne field in the Danish sector of the Southern Central Graben of the North Sea. The maximum offset was 4200m, providing sufficient velocity resolution at target depth (~3000m) with a reasonable frequency spectrum (~60Hz). We can see an area with a benign flat lying overburden, below which compressional deformation and structural inversion throughout the Cretaceous has resulted in a structural high at the level of the Chalk reservoir sequence (figure 1). The chalk sequence thins over this elongate anticlinal ridge and asymmetrically thickens off-structure with a thicker chalk sequence developed to the right (West) of the ridge. Above the structure, gas leakage gives rise to brightening of the seismic image.

The model building and migration for the exploration project was performed isotropically using iterative CRP scanning with a layered model incorporating the top and base chalk as the main velocity contrasts, with a single compaction gradient within the chalk (figure 2). Both the thin and the thick chalk sequences were represented by a single layer, as the intermediate intra-chalk horizons were discontinuous. With hindsight, it would have been better to include a layer within the thick chalk sequence to account for the changes in the compaction gradient regime.

Upon completion of the exploration preSDM with layered model building, a gridded update (Hardy, 2003) was employed to investigate detailed changes within the chalk for production purposes. The portion outlined in the box on figure 2, is used for the detaile shown in later figures.

For the gridded tomography, we employ an automated continuous autopicker, described by Hardy (2003).

Whereas the exploration 3D preSDM project was isotropic, the more detailed production 3D preSDM (which employed the gridded tomography) was anisotropic (Thomsen, 1986). Hence to facilitate a fairer comparison, we have re-run the gridded model building isotropically, but on a 2D crestal line over the reservoir structure to exemplify the procedures involved in the 3D gridded tomography. Consequently, all the figures shown here, except figure 1, are the results of isotropic 2D preSDM, with either the layer-based 3D model or a 2D gridded tomographic model.

Figure 3 shows the result of three iterations of gridded tomography: for the most-part, the velocity remains unchanged down to the top chalk, other than for the introduction of a low velocity zone which corresponds to the gas bright spots. Within, and just below the chalk however, we see dramatic changes in the velocity. To the right of the crestal ridge, the simple compaction gradient is replaced by a more complex regime, and to the left of the ridge, we see the introduction of a low velocity layer below the chalk, feeding up into the crestal structure.

We observe that the upper part of the chalk is better described by a near-constant velocity region, and that the strong gradient regime commences deeper within the chalk. Importantly, the vertical compaction gradient is not constant laterally across the chalk body: when building a layered model, it is usual to keep a constant gradient in a given layer, as we seldom have sufficient well control to justify lateral variation in layered models.

In figure 4 shows an enlargement of the zone within the box (figures 2 & 3) for the layered and gridded velocity models, and in figure 5, we have the corresponding preSDM images. The structure below the chalk is much better defines using the gridded model. Doubtless, a comparable result could be achieved using a layered model, if much more time and effort was put into the layered model building.

Figure 6 shows a selection of CRP gathers from this zone for the layered and gridded models. It is clear that the events corresponding to the gas bright spots above the crestal ridge are over-migrated in the layered model, as the localized low-velocity anomaly was not included in the layered model. This would probably be impractical due to the highly localized nature of the anomaly. However, in the gridded results, the gas leakage anomaly is detected by the autopicking and gridded tomography.

Figures 7-9 show some of the intermediate QC products from the autopicking and tomography. Figure 7 shows the residual curvature field picked from the migrated CRP gathers, after the second iteration of migration. After tomographic update and subsequent remigration, the overall residual curvature (as found by the subsequent picking) is reduced, and errors consigned to ever deeper parts of the model (figure 8). Figure 9 shows the coherency of the picks found by the autopicker. These spatial (and offset) coherency values can by used as a constraint in the inversion.

The final comparisons of the preSDM images with the superimposed velocity models are shown in figures 10 & 11.

Discussion

We have addressed strategies for building models for complex chalk geology, and contrasted results for manual update in a layered model building scheme, with a dense auto-picking-driven gridded tomographic approach. Although it should be possible to achieve a detailed model building procedure using a layered approach, it has proven to be more practical to use the gridded strategy when we have subtle variations in the velocity structure.

A smooth starting model which generally follows the overall velocity trend is useful as a starting point for the gridded approach. If we are too far from the actual model, then the autopicker may have difficulty following the residual moveout in the migrated CRP gathers, especially if the curvature in the gathers is aliased.

However, if the starting velocity model is not sufficiently smoothed, then the gridded tomography will have difficulty introducing the required changes at high velocity contrast boundaries (such as at the top chalk) which are initially in error.

For these data, and on several other projects, we have noted the gridded tomography is a viable approach to model building in areas hitherto considered only suitable for a layered approach.

Background Reading

Al-Chalabi, M., 1974, An analysis of stacking, rms, average, and interval velocities of horizontally layered ground. Geophys. Prosp., 22, 458-475.

Alkhalifah, T., & Tsvankin, I., 1995, Velocity analysis for transversely isotropic media; Geophysics, 60, no.5, 1550-1566.

Alkhalifah, T., 1997, Velocity analysis using nonhyperbolic moveout in transversely isotropic media; Geophysics, 62, no.6, 1839-1854.

Hardy, P.B., 2003, High resolution tomographic MVA with automation, SEG/EAGE summer research workshop, Trieste.

Hawkins, K., Leggot, R., Williams, G., & Kat, H., 2001, Addressing anisotropy in 3D pre-stack depth migration: a case study from the Southern North Sea. The Leading Edge, v20, No.5, pp528-543.

Jones, I.F., 2003, A review of 3D preSDM velocity model building techniques First Break, v21, No.3, pp45-58.

Jones, I.F., Bridson, M.L., & Bernitsas, N.X., 2003b, Anisotropic Ambiguities in TI Media. First Break, v21, No.4, pp31-37.

Thomsen, L, 1986, Weak elastic anisotropy; Geophysics, 51, no.10, 1954-1966.

Acknowledgements

The authors wish to thank the Amerada Hess UK, and partners for kind permission to use their data

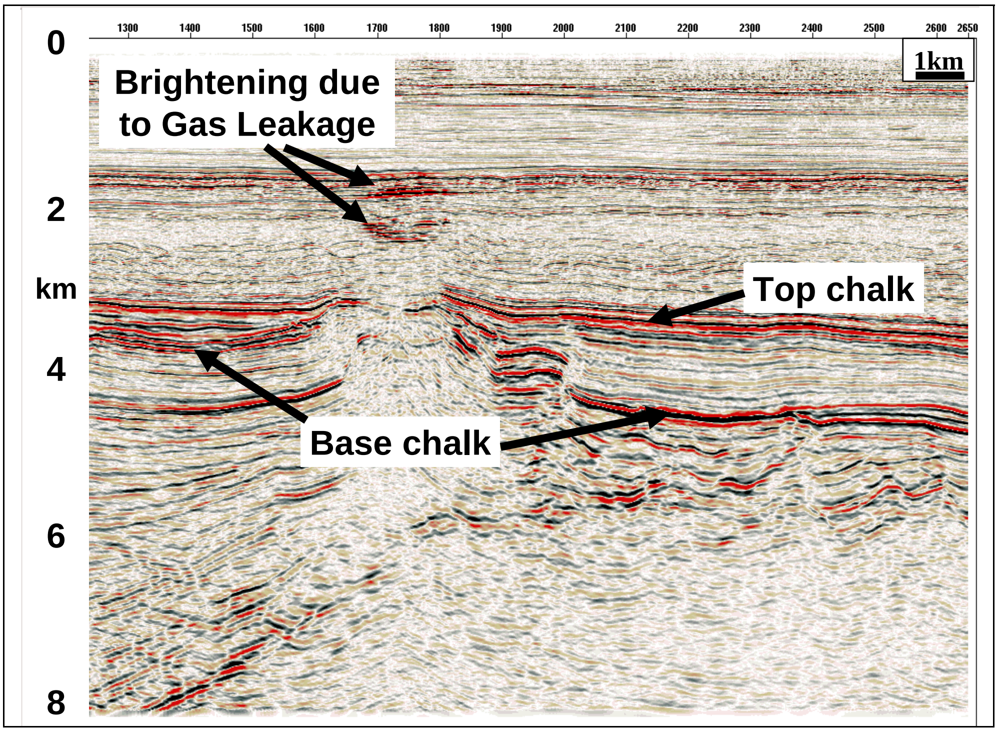

Figure 1: 3D preSDM image using a layered model: a benign overburden over a complex chalk layer

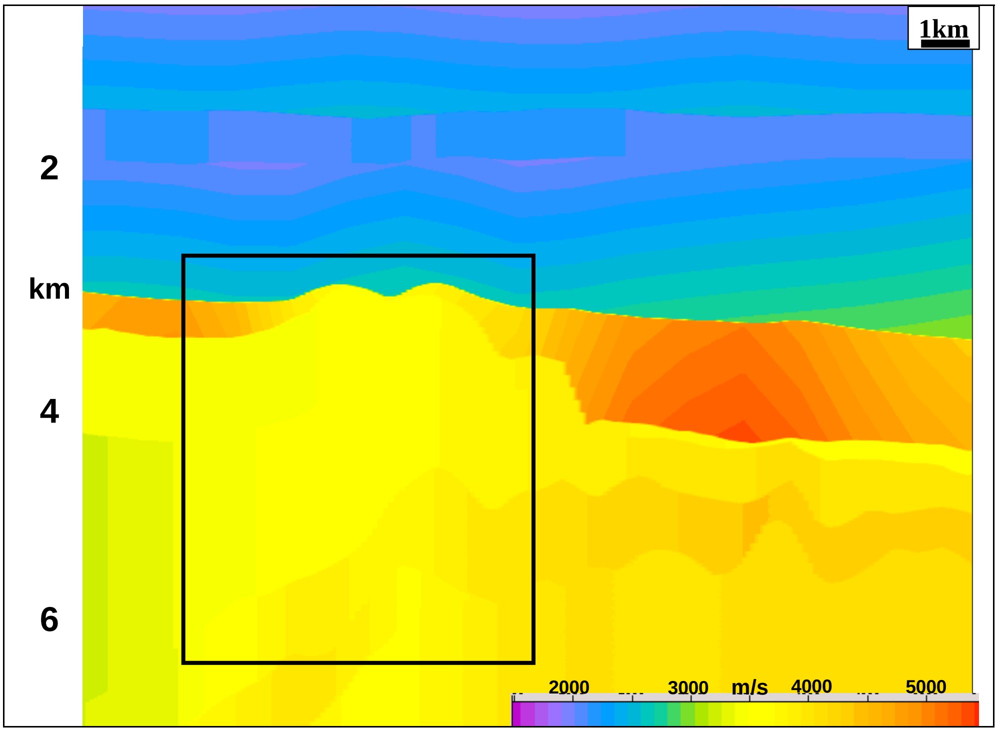

Figure 2: The exploration project 3D layered model used to create the preSDM image in figure.1.

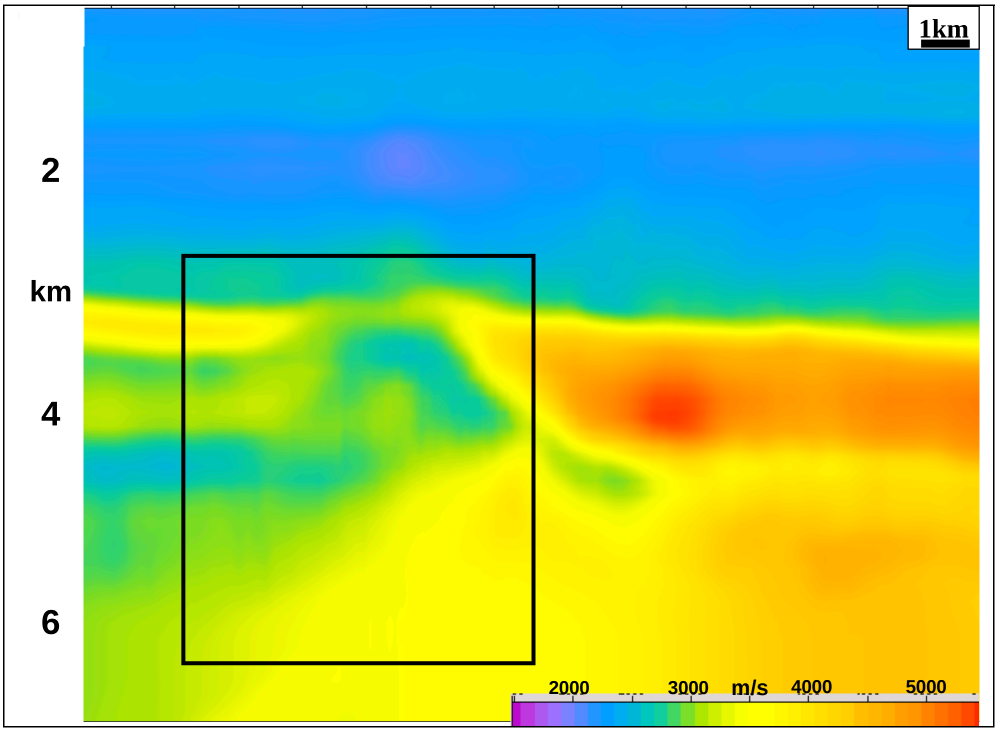

Figure 3: The 2D gridded tomographic model (after 3 iterations). A plane wave destructor autopicker was used to track horizon segments and determine the degree of residual moveout. This information, in conjunction with weights from the plane-wave fitting is input to the tomography.

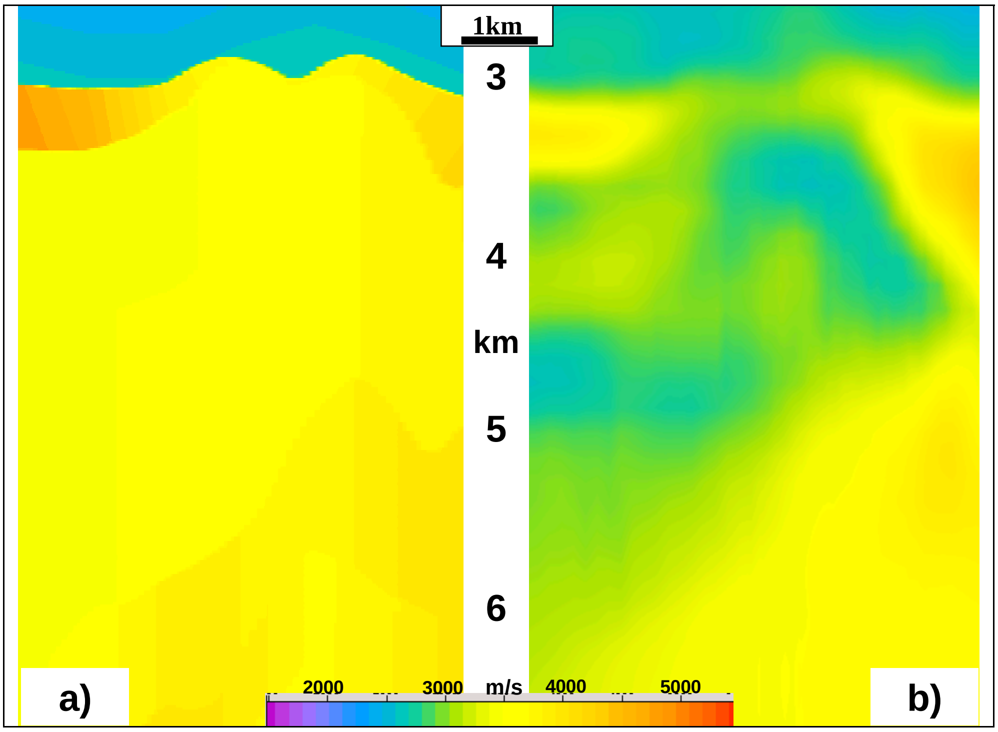

Figure 4: Detail from box (shown in fig. 3): a) layered model; b) gridded model

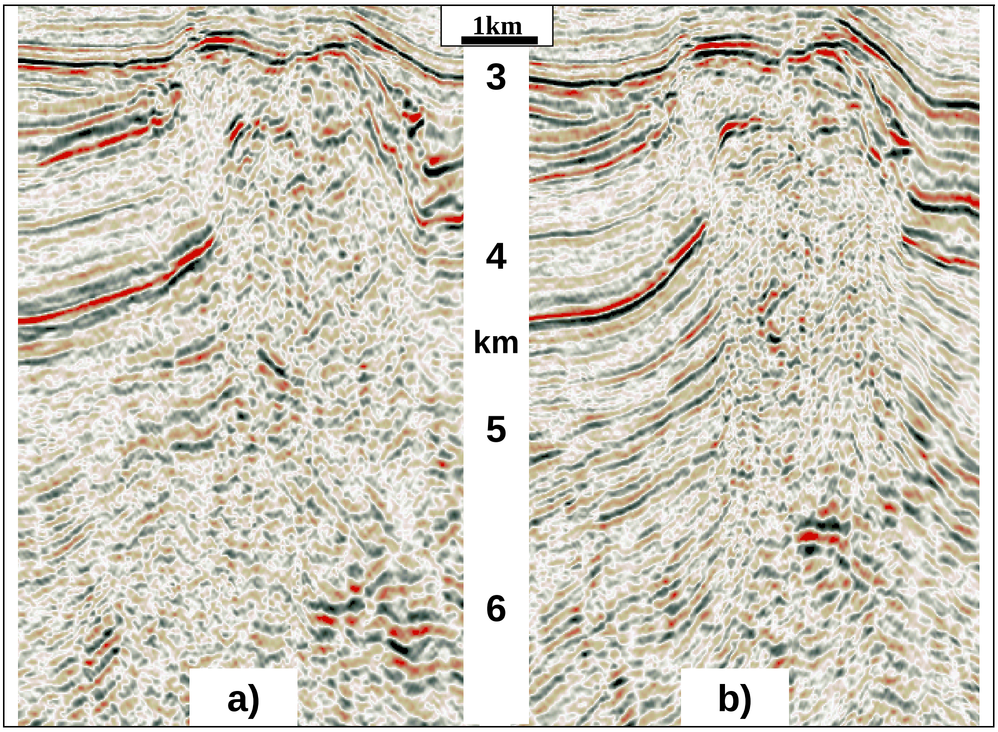

Figure 5: Detail from box (shown in fig. 3): a) 2D preSDM from layered model; b) 2D preSDM from gridded model after 3 iterations

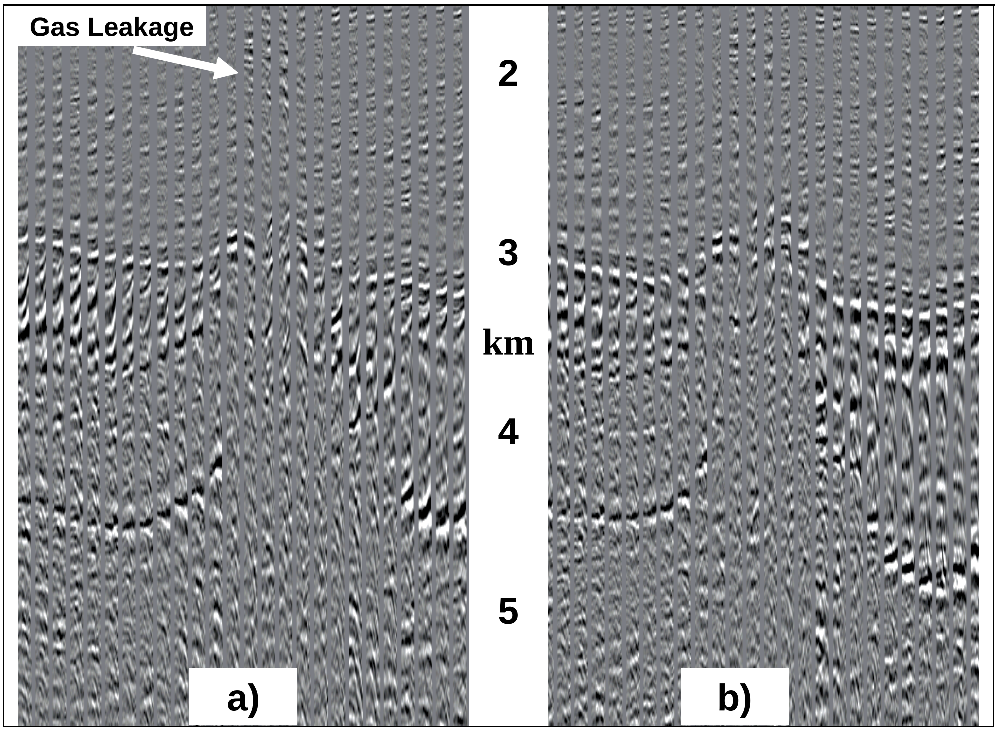

Figure 6: Detail from box (shown in fig. 3): events in the low velocity gas leakage zone are over-migrated in the layered model preSDM (a) but corrected in the gridded model preSDM (b)

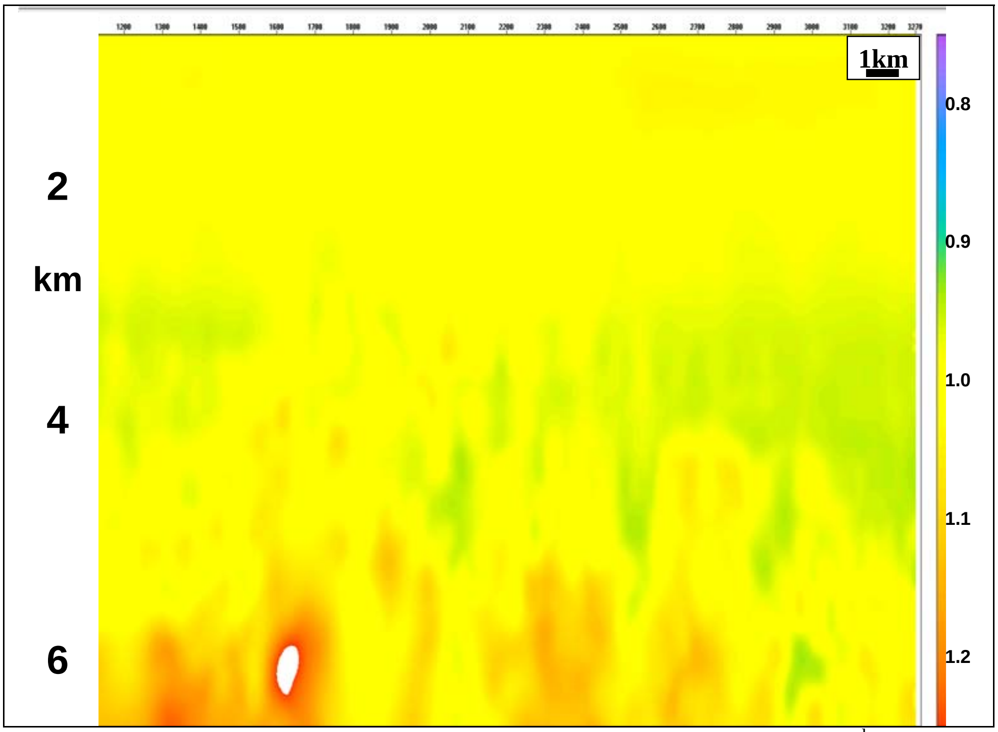

Figure 7: Hyperbolic curvature after migration iteration 2, as input to 3rd iteration of gridded tomography. These values are derived by the plane-wave destructor autopicker. At each location along the line, and each depth, events which show spatial coherence are analysed to measure their local in-line dip, coherence, and residual offset curvature. The curvature can be characterized either non-hyperbolically (general fit), or hyperbolically, as used in this example. The scale is shown as the velocity perturbation required to flatten the gather (values <1 indicate velocity too slow, values >1 indicate velocity too high).

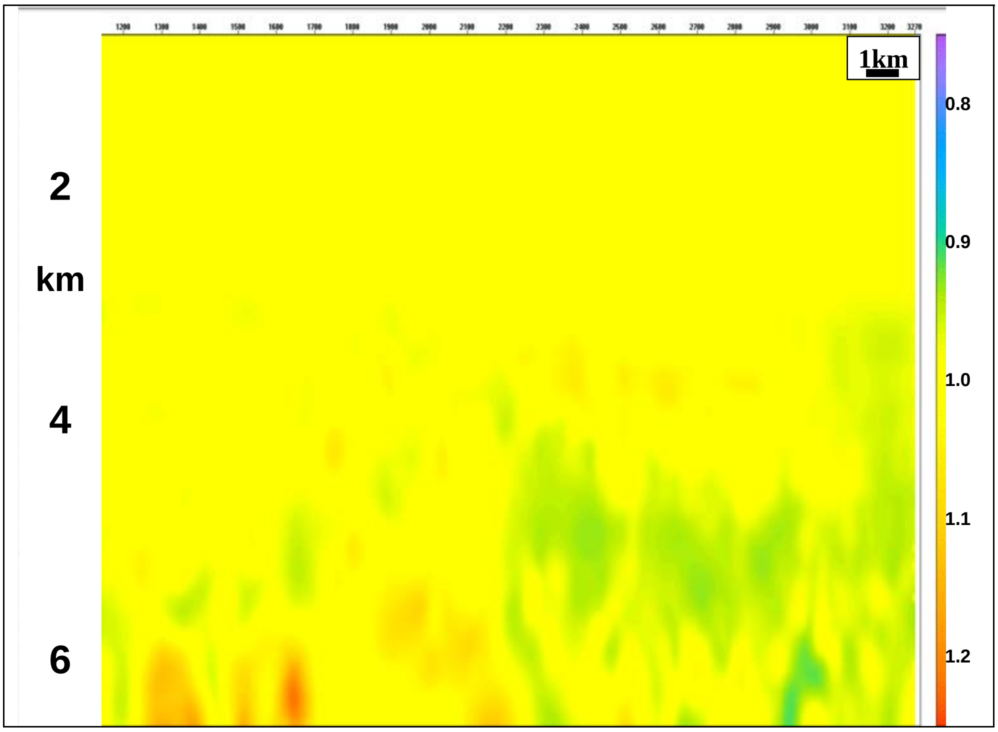

Figure 8: Hyperbolic curvature after migration iteration 3, after update by gridded tomography. Errors are reduced overall, and those that remain appear in deeper parts of the model

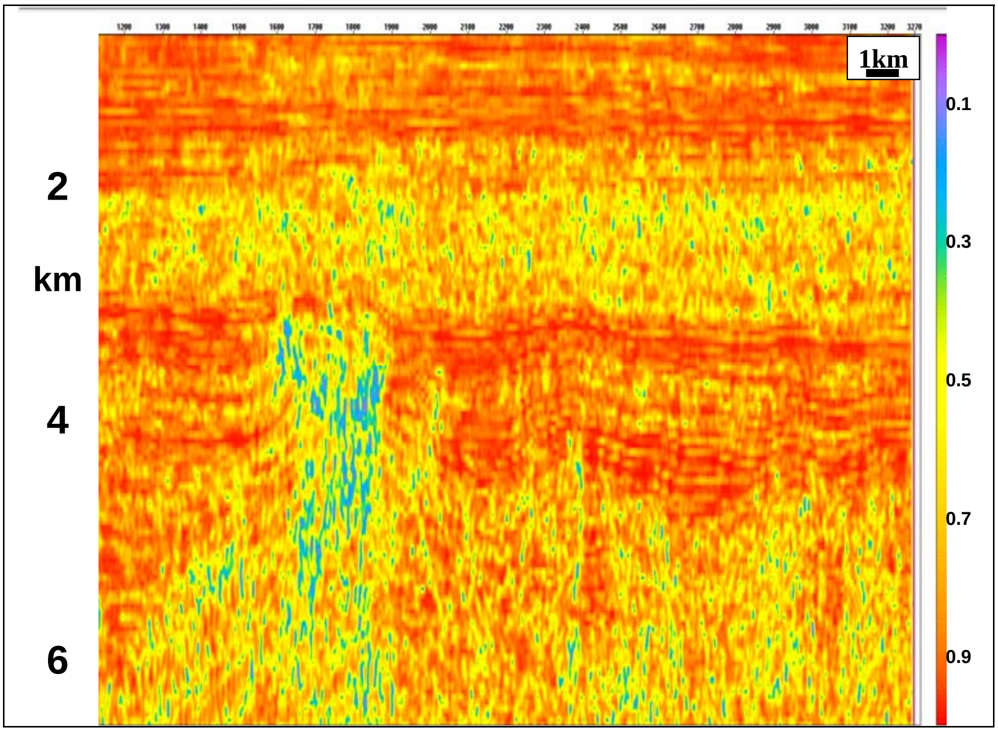

Figure 9: Coherency measure determined after iteration 3. The coherency of the event segments is used to weight the tomographic inversion. A value of 1 indicates perfect coherence, low numbers indicate poor coherence).

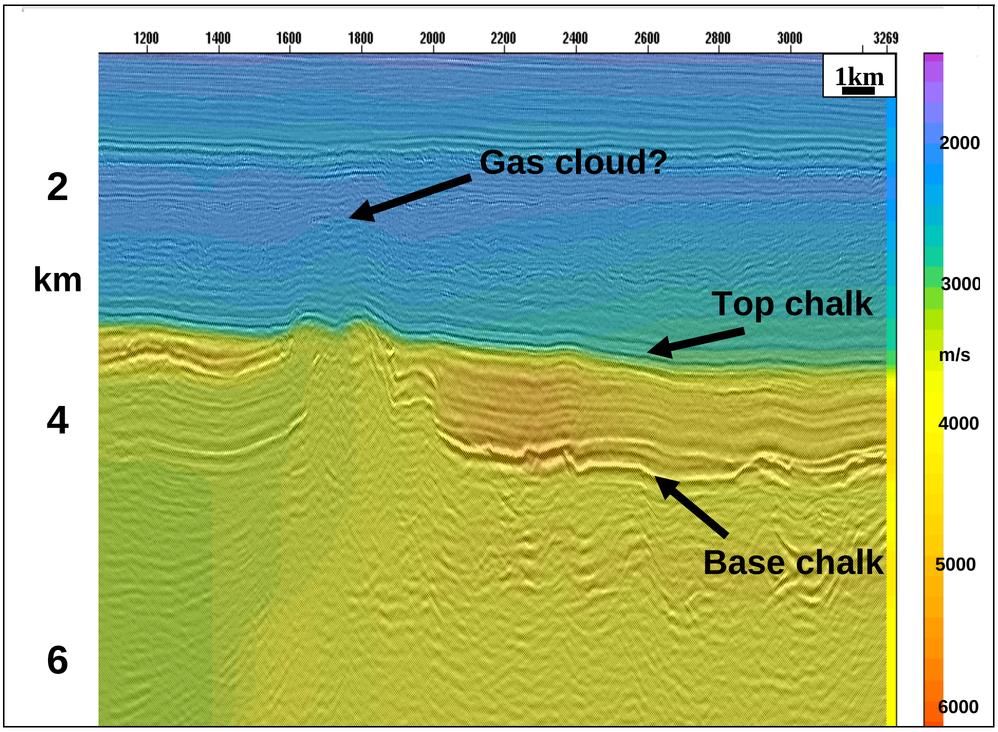

Figure 10: 2D preSDM with the 3D layered model, with velocity overlay

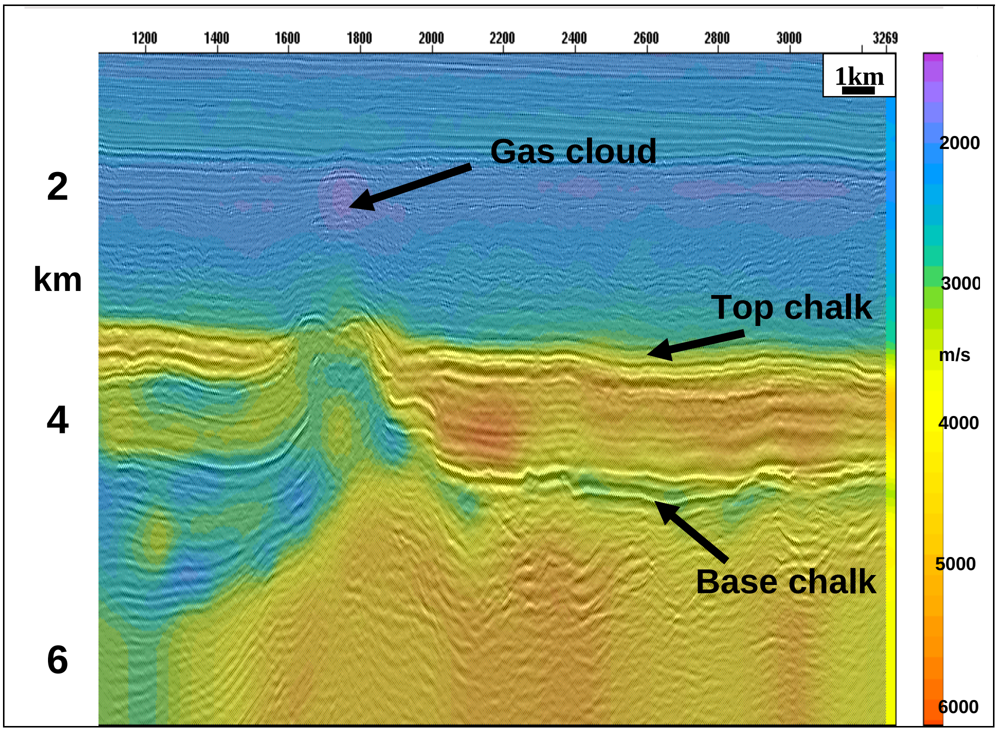

Figure 11: 2D preSDM with the final 2D gridded model, with velocity overlay